Supplementary Information

Elucidating the correlation between the prelithiation concentration of a Li_xSi anode and performance of all-solid-state lithium–sulfur batteries

Min Ju Kim, Yu Hong Jeong, Sung Kang, Jungjae Park, Jung Hoon Song, Tae Ho Shin and Hyung-Tae Lim*

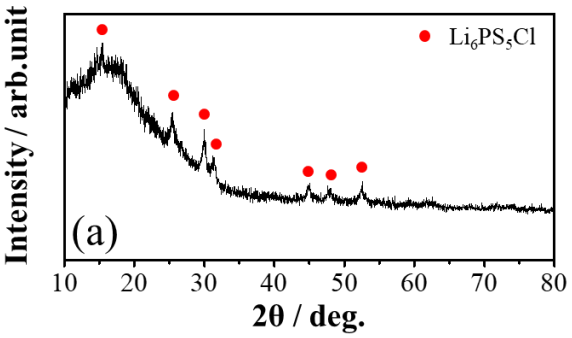
Intensity / arb.unit
Li6PS5Cl
(a)
10 20 30 40 50 60 70 80
2θ / deg.

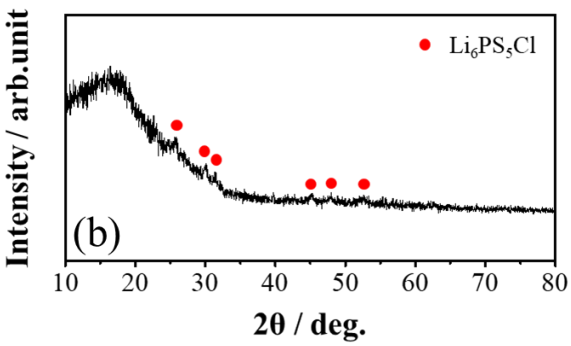
Intensity / arb.unit
Li6PS5Cl
(b)
10 20 30 40 50 60 70 80
2θ / deg.

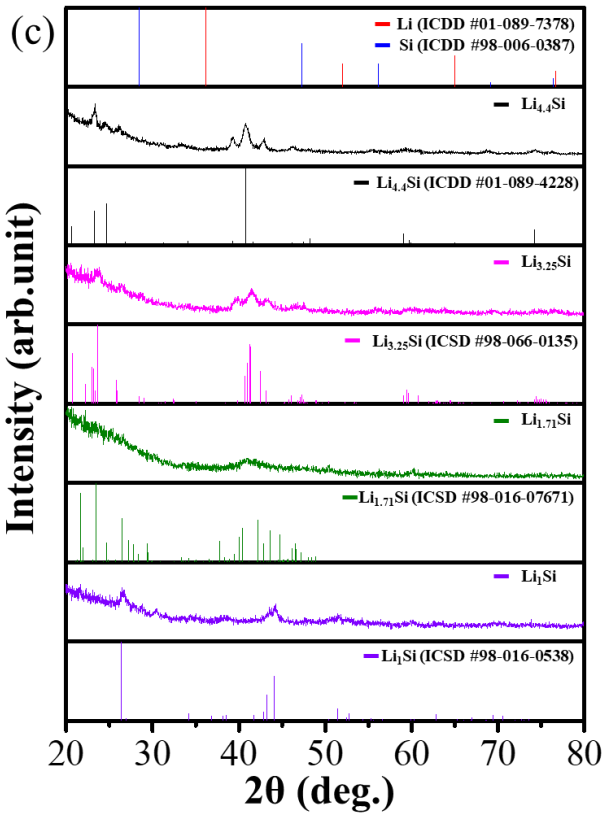
(c)
Li (ICDD #01-089-7378)
Si (ICDD #98-006-0387)
Li4.4Si
Li4.4Si (ICDD #01-089-4228)
Li3.25Si
Li3.25Si (ICSD #98-066-0135)
Li1.71Si
Li1.71Si (ICSD #98-016-07671)
LiSi
LiSi (ICSD #98-016-0538)
Intensity (arb.unit)
20 30 40 50 60 70 80
2θ (deg.)

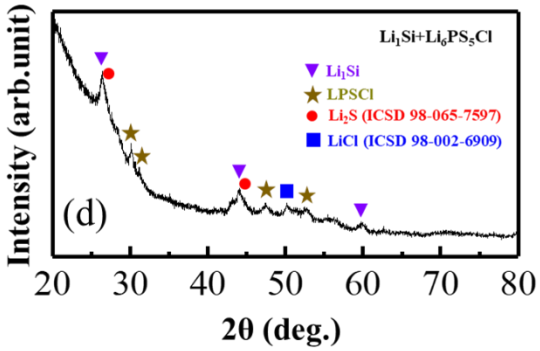
LiSi+Li6PS5Cl
LiSi
LPSCl
Li2S (ICSD 98-065-7597)
LiCl (ICSD 98-002-6909)
Intensity (arb.unit)
(d)
20 30 40 50 60 70 80
2θ (deg.)

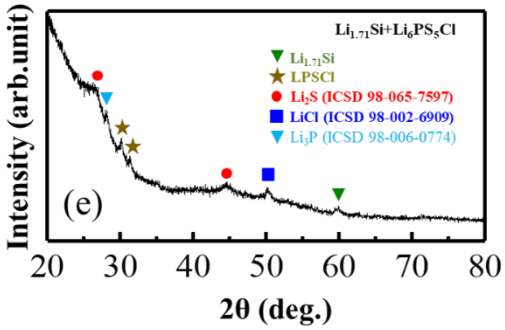
Li1.71Si+Li6PS5Cl
Li1.71Si
LPSCl
Li2S (ICSD 98-065-7597)
LiCl (ICSD 98-002-6909)
Li3P (ICSD 98-006-0774)
Intensity (arb.unit)
(e)
20 30 40 50 60 70 80
2θ (deg.)

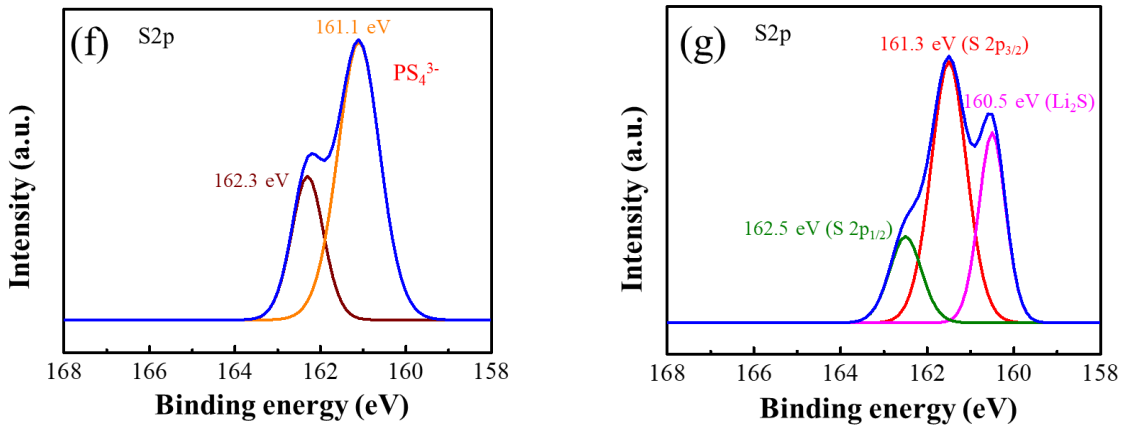

Fig. S1 X-ray diffraction patterns of (a) Li_6PS_5Cl (LPSCl; solid electrolyte), (b) sulfur composite cathode, (c) Li_xSi (x = 1.0, 1.17, 3.25, and 4.4), (d) $Li_{1.0}Si$+LPSCl, and (e) $Li_{1.71}Si$+LPSCl powders obtained after planetary ball milling; X-ray photoelectron spectroscopy spectra of (f) a pristine LPSCl pellet and (g) the LPSCl SE surface detached from a $Li_{1.71}Si$ anode cell.

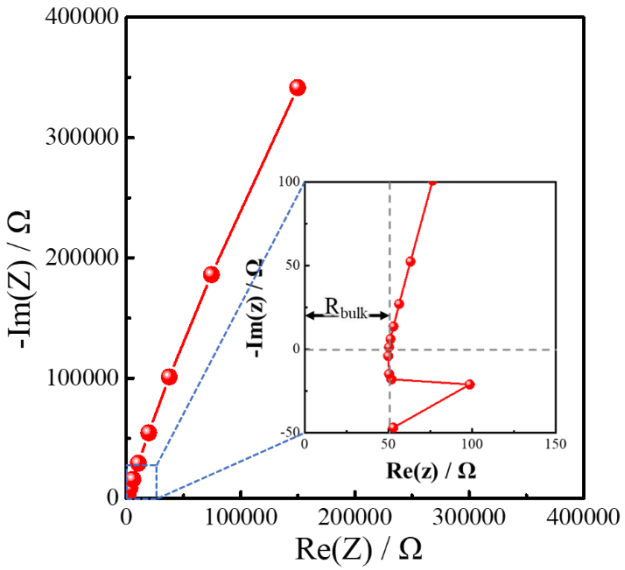

Fig. S2 Impedance spectrum of an LPSCl disk.

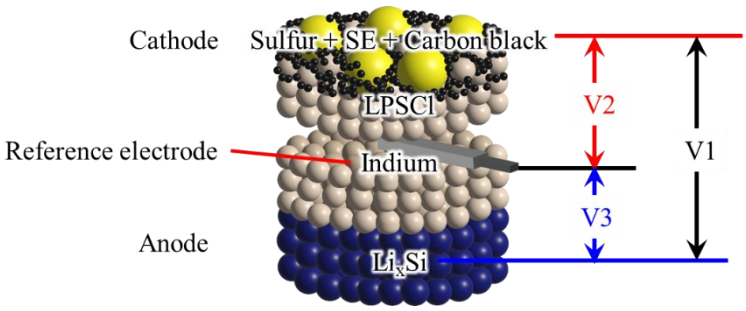

Fig. S3 Schematic of the three-electrode cell fabricated in this study and measured potentials (V1, V2, V3).

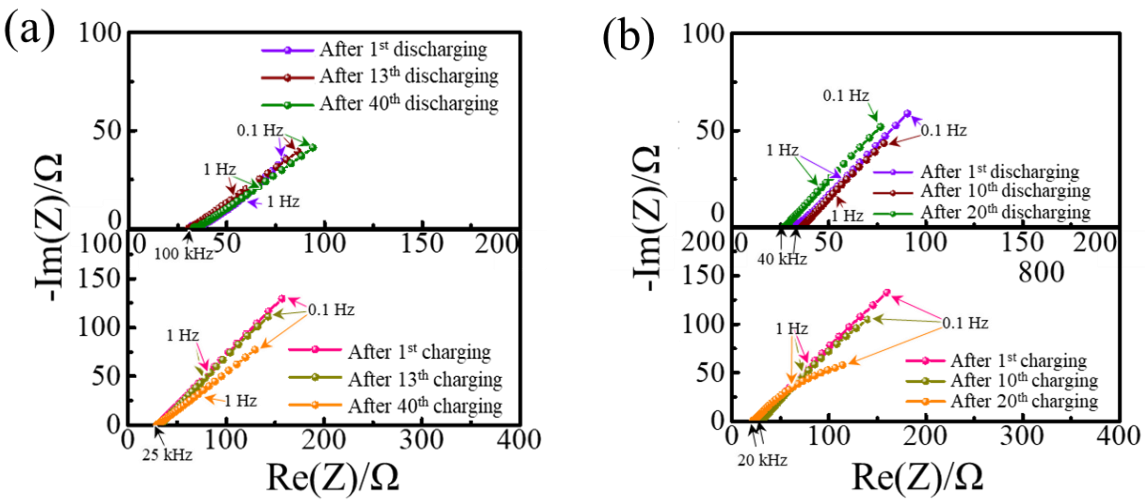

Fig. S4 Impedance spectra of cells with a $Li_{3.25}Si$ anode and (a) an anode-to-cathode capacity (N/P) ratio of 3.89 recorded after the first, 13th, and 40th discharge (charge) and (b) an N/P ratio of 3.0 recorded after the first, 10th, and 20th discharge (charge).

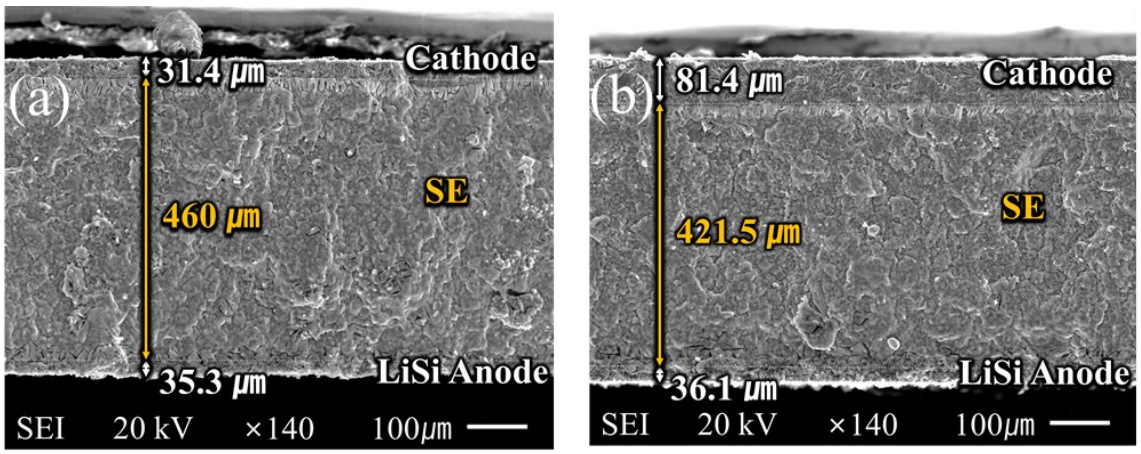

Fig. S5 Scanning electron microscopy (SEM) images of cross-sectioned cells with a $Li_{1.0}Si$ anode and N/P ratios of (a) 3.89 and (b) 1.2.

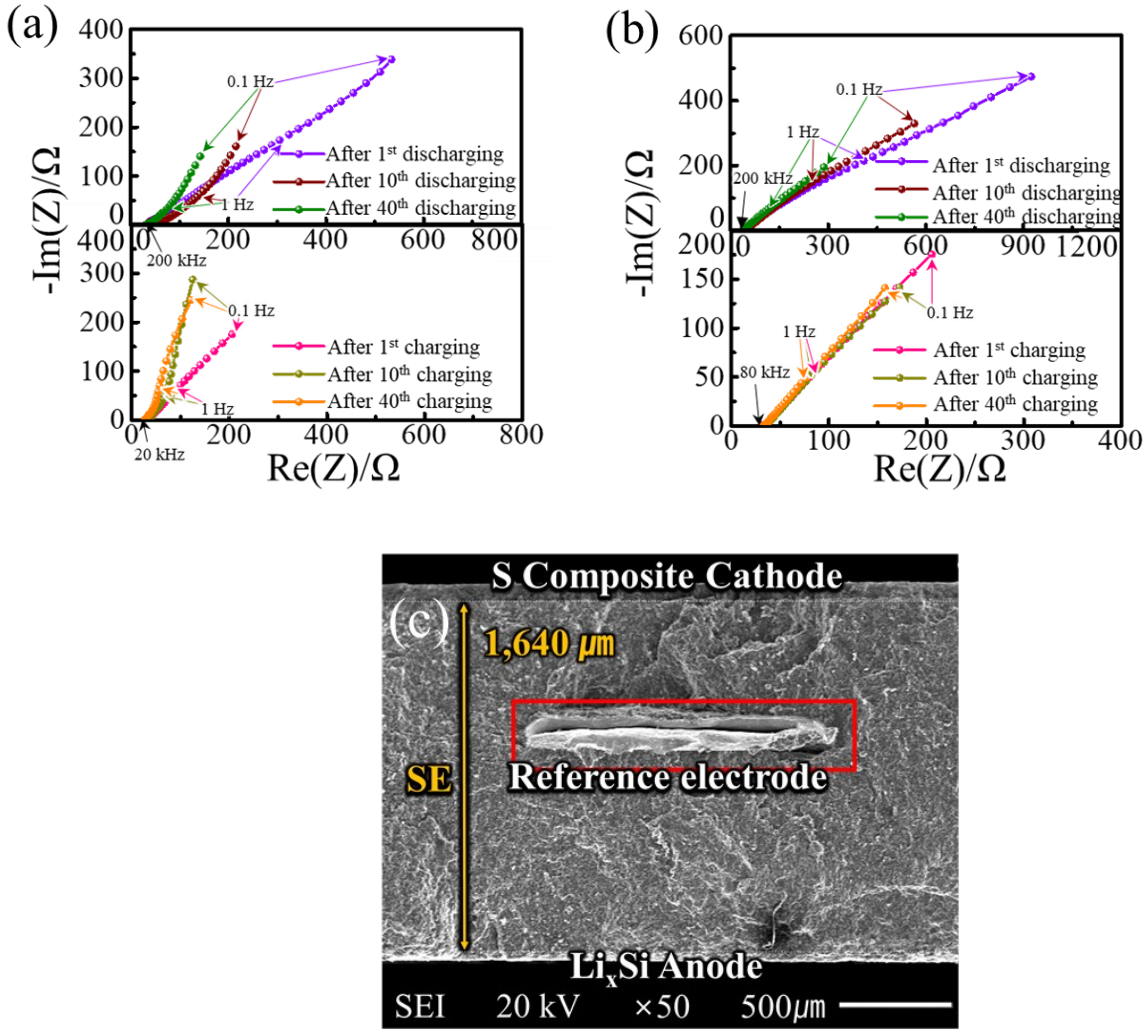

Fig. S6 Impedance spectra of cells with a $Li_{1.0}Si$ anode and N/P ratios of (a) 3.89 and (b) 1.2 recorded after the first, 10th, and 40th discharge (charge). (c) Cross-sectional SEM image of a three-electrode $Li_{1.0}Si$ anode cell with an N/P ratio of 1.2.

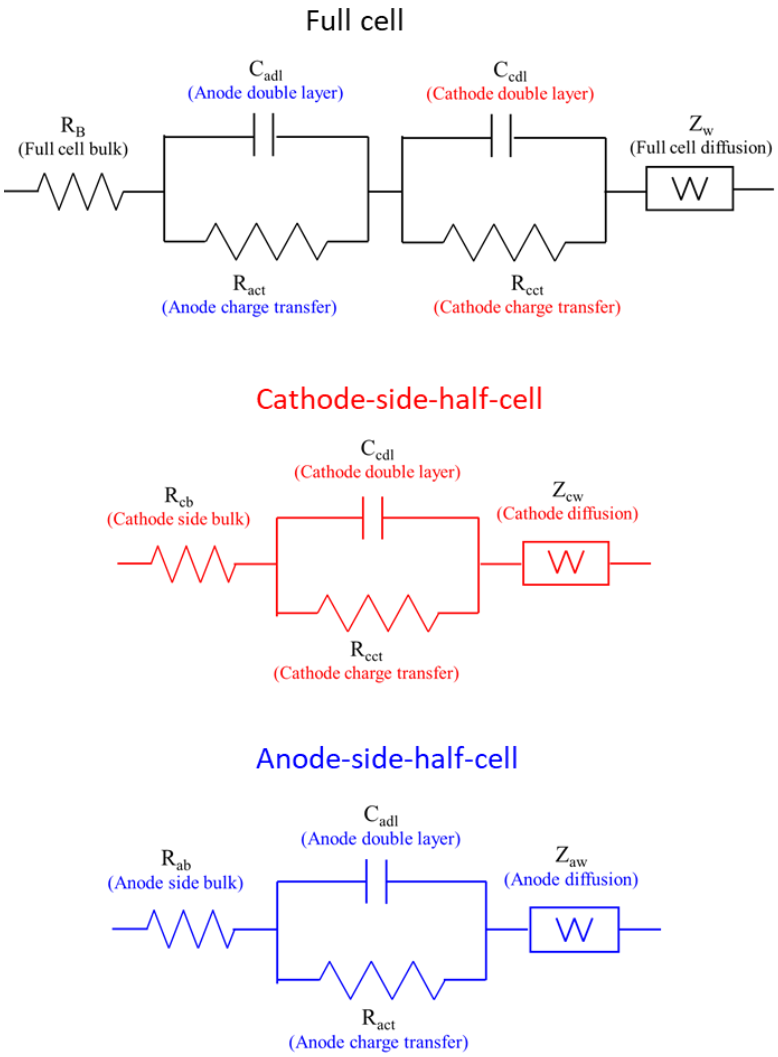

Fig. S7 Equivalent circuit models for the full cell (V1), cathode-side half-cell (V2), and anode-side half-cell (V3) of a three-electrode cell.

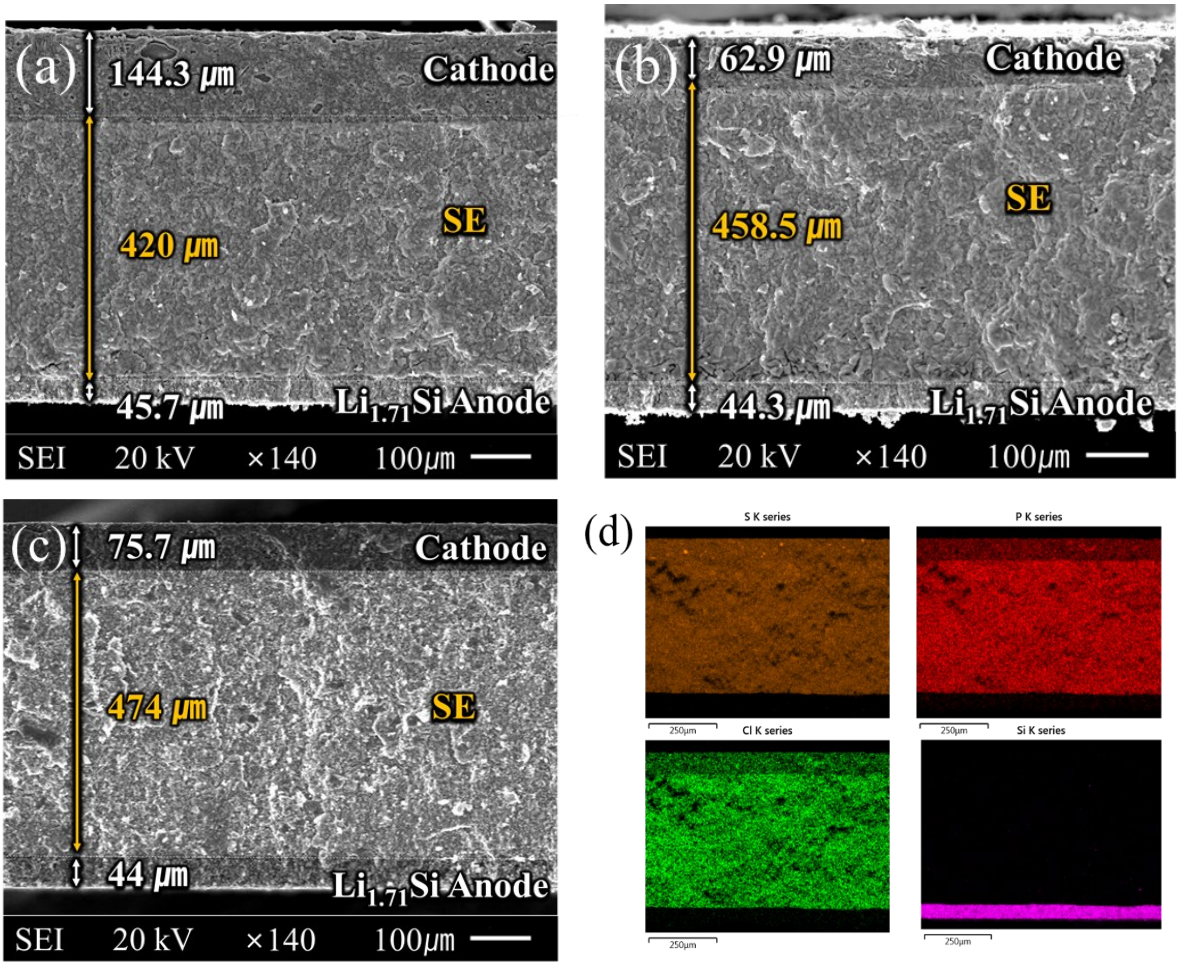

Fig. S8 Cross-sectional SEM images of $Li_{1.71}Si$ anode cells with N/P ratios of (a) 1.2, (b) 3.89, and (c) 2.05. (d) S, P, Cl, and Si distributions from the energy-dispersive X-ray spectroscopy (EDS) mapping of (c).

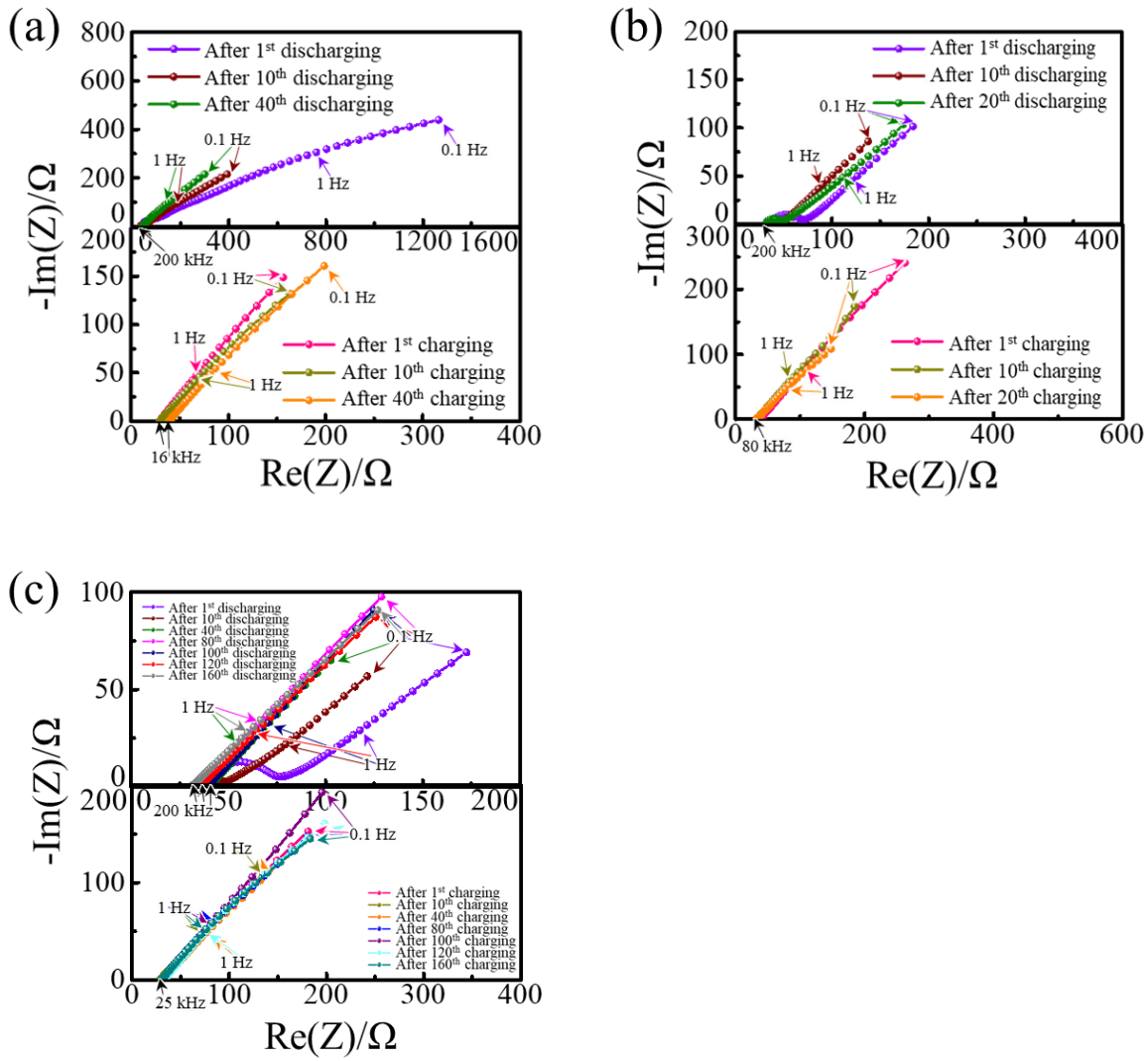

Fig. S9 Impedance spectra of $Li_{1.71}Si$ anode cells with (a) an N/P ratio of 1.2 recorded after the first, 10th, and 40th discharge (charge), (b) an N/P ratio of 3.89 recorded after the first, 10th, and 20th discharge (charge), and (c) an N/P ratio of 2.05 recorded after the first, 10th, 40th, 80th, 100th, 120th, and 160th discharge (charge).

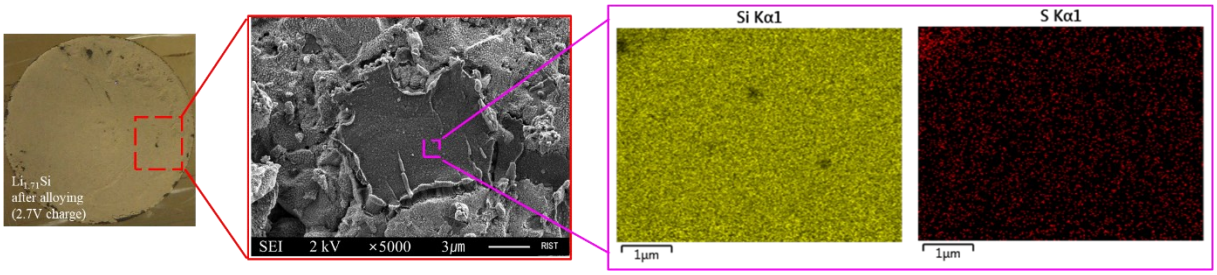

Fig. S10 Digital microscopy (left) and SEM–EDS images (middle and right) of the solid electrolyte surface detached from the $Li_{1.71}Si$ anode cell (N/P ratio = 2.05) cycle-tested at a constant current of 1000 μA for 17 cycles.

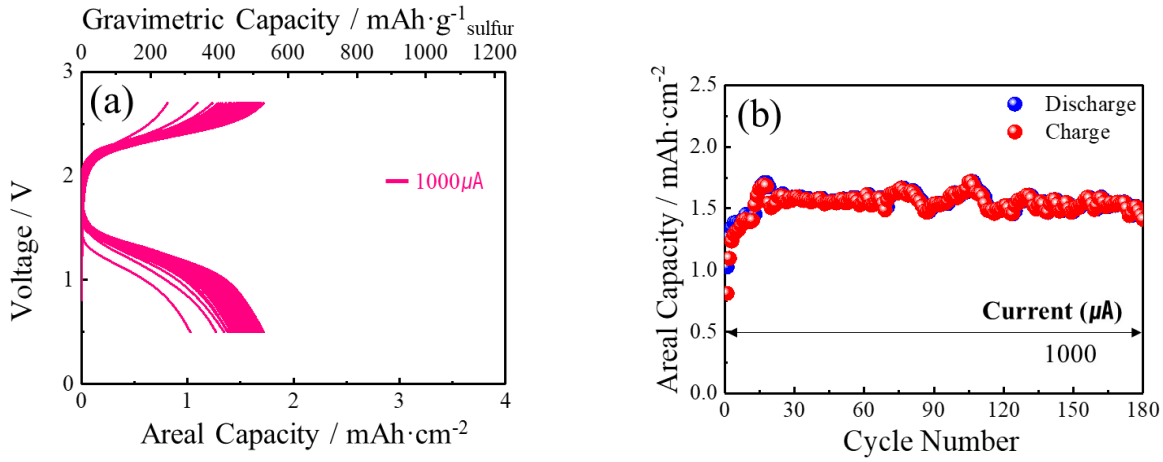

Fig. S11 (a) Discharge–charge curves and (b) areal capacity–cycle number plots of the $Li_{1.71}Si$ anode cell (N/P ratio = 2.05) cycle-tested at a constant current of 1000 μA for 180 cycles.

Table S1. N/P ratios and mass loadings of the cathode and anode active materials in cells with different Li_xSi anodes (x = 1.0, 1.71, and 3.25).

Li_xSi	N/P ratio	Mass loading of cathode active material [mg/cm^2]	Mass loading of anode active material [mg/cm^2]
Li_1Si	1.2	3.25	6.49
	3.89	1.01	6.49
$Li_{1.71}Si$	1.2	5.52	6.49
	2.05	3.25	6.49
	3.89	1.79	6.49
$Li_{3.25}Si$	3.89	3.25	6.49
	3	4.22	6.49

Table S2. Mechanical alloying conditions used to prepare Li_xSi (x = 1.0, 1.71, 3.25, and 4.4).

Li_xSi	BPR	Rotation speed [rpm]	Milling time [h]
Li_1Si	330:1	370	30
$Li_{1.71}Si$	330:1		30
$Li_{3.25}Si$	110:1		2.5
$Li_{4.4}Si$	110:1		2.5